A completely new click chemistry ...

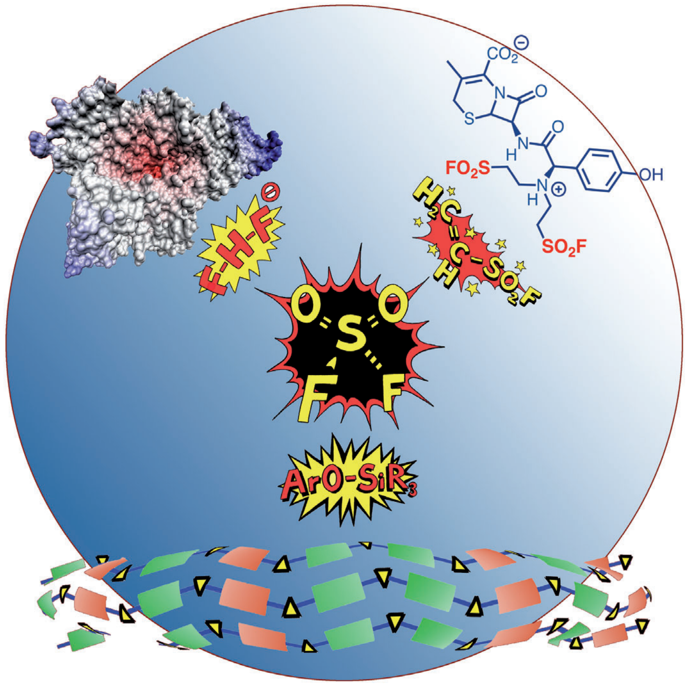

... is described by K. B. Sharpless, M. G. Finn, and co-workers in their Review on page 9430 ff. The robust bond between S^{VI} and F atoms (such as in the gas SO_2F_2 and Michael acceptor $HC{=}CHSO_2F$) can be specifically activated by proton (often in the form of the bifluoride ion, HF_2^-) or silicon centers (e.g. an aryl silyl ether) to create S–heteroatom linkages of surprising stability. Applications of this click 2.0 method to the synthesis of small molecules or polymers (see the Communication by K. B. Sharpless, V. V. Fokin et al. on page 9466 ff.), and the modification of biomolecules—each represented at the periphery of the image—are discussed.

Tandem Peptide Cyclization

A. Friedler et al. describe in their Communication on page 9450 ff. a tandem strategy involving in situ deprotection, cyclization, and trifluoroacetic acid cleavage for the solid-phase cyclization of peptides under highly acidic conditions.

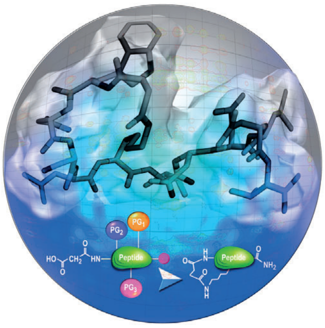

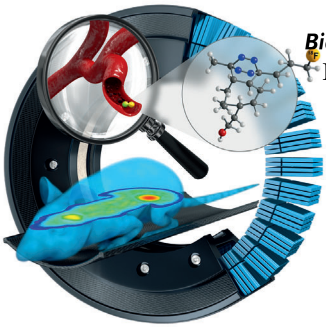

Bioorthogonal Imaging

H. Mikula, C. Kuntner, et al. describe the synthesis and application of a low-molecular-weight radiolabeled tetrazine derivative in their Communication on page 9655 ff. This compound is a suitable reagent for pretargeted PET imaging.

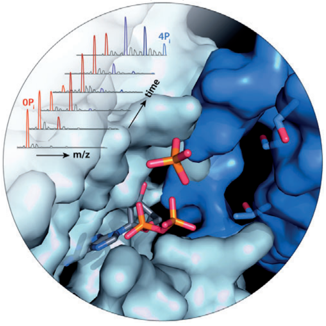

Protein Mass Spectrometry

Multiple aspects of protein phosphorylation can be examined simultaneously by a combination of native and "bottom-up" mass spectrometry. This method is described by A. J. R. Heck et al. in their Communication on page 9660 ff.

How to contact us:

Editorial Office:
E-mail: angewandte@wiley-vch.de
Fax: (+49) 6201–606-331
Telephone: (+49) 6201–606-315

Reprints, E-Prints, Posters, Calendars:
Carmen Leitner
E-mail: chem-reprints@wiley-vch.de
Fax: (+49) 6201–606-331
Telephone: (+49) 6201–606-327

Copyright Permission:
Bettina Loycke
E-mail: rights-and-licences@wiley-vch.de
Fax: (+49) 6201–606-332
Telephone: (+49) 6201–606-280

Online Open:
Margitta Schmitt, Carmen Leitner
E-mail: angewandte@wiley-vch.de
Fax: (+49) 6201–606-331
Telephone: (+49) 6201–606-315

Subscriptions:
www.wileycustomerhelp.com
Fax: (+49) 6201–606-184
Telephone: 0800 1800536 (Germany only)
+44(0) 1865476721 (all other countries)

Advertising:
Marion Schulz
E-mail: mschulz@wiley-vch.de
jspiess@wiley-vch.de
Fax: (+49) 6201–606-550
Telephone: (+49) 6201–606-565

Courier Services:
Boschstrasse 12, 69469 Weinheim

Regular Mail:
Postfach 101161, 69451 Weinheim

Angewandte Chemie International Edition is a journal of the Gesellschaft Deutscher Chemiker (GDCh), the largest chemistry-related scientific society in continental Europe. Information on the various activities and services of the GDCh, for example, cheaper subscription to *Angewandte Chemie International Edition*, as well as applications for membership can be found at **www.gdch.de** or can be requested from GDCh, Postfach 900440, D-60444 Frankfurt am Main, Germany.

GDCh
GESELLSCHAFT
DEUTSCHER CHEMIKER

Service

Author Profile

"If I were not a scientist, I would be a businessman. I can never resist the taste of success. …"
This and more about Mohammad K. Nazeeruddin can be found on page 9419.

News

H. Hopf

H.-U. Reissig

P. S. Baran

M. Inoue

M. D. Burke

Meeting Review

The Bürgenstock Conference on Stereochemistry was founded in 1965 by André S. Dreiding (see picture) who passed away in December 2013. In their Meeting Review, Tanja Gulder and Tobias A. M. Gulder summarize the 49th Bürgenstock Conference, which took place in May 2014.

Books

Highlights

C–H Activation

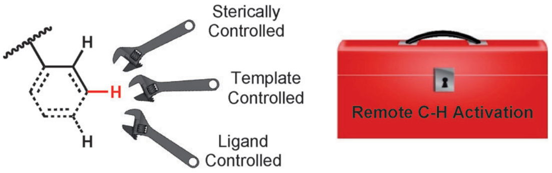

Novel tool set: New methodologies for the functionalization of remote C–H bonds have been developed recently. In diverse approaches high selectivities are achieved for the functionalization of less reactive C(sp^2)–H as well as C(sp^3)–H bonds distal to any substituents.

Reviews

Click Chemistry

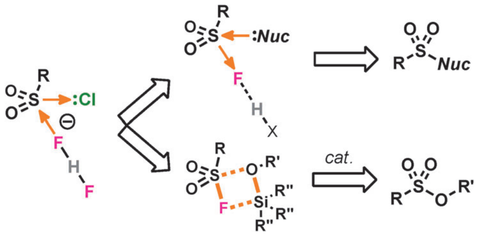

Old chemistry in new glory: Sulfonyl fluoride exchange (SuFEx) forges rugged inorganic links between carbon centers. Like most click reactions, it is an old process now improved to allow the underappreciated sulfate connection to be made for a variety of purposes. The various exchange events uniquely enabled by the use of fluoride are highlighted here in orange.

Communications

Tandem Peptide Cyclization

A new approach for solid-phase peptide cyclization under highly acidic conditions involves tandem in situ deprotection, cyclization, and trifluoroacetic acid cleavage (see scheme). The cyclization occurs between a lysine side chain and a succinic acid derivative at the peptide N-terminus and proceeds via a highly active succinimide intermediate, which was isolated and characterized.

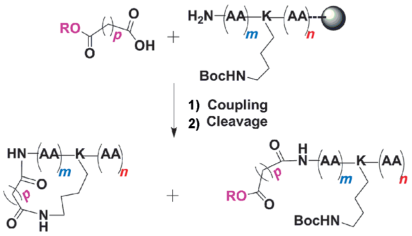

For the USA and Canada: ANGEWANDTE CHEMIE International Edition (ISSN 1433-7851) is published weekly by Wiley-VCH, PO Box 191161, 69451 Weinheim, Germany. US mailing agent: SPP, PO Box 437, Emigsville, PA 17318. Periodicals postage paid at Emigsville, PA. US POSTMASTER: send address changes to *Angewandte Chemie*, John Wiley & Sons Inc., C/O The Sheridan Press, PO Box 465, Hanover, PA 17331. Annual subscription price for institutions: US$ 11.738/10.206 (valid for print and electronic / print or electronic delivery); for individuals who are personal members of a national chemical society prices are available on request. Postage and handling charges included. All prices are subject to local VAT/sales tax.

Rotational Intergrowth

M. Khaleel, A. J. Wagner, K. A. Mkhoyan, M. Tsapatsis* ______ **9456 – 9461**

On the Rotational Intergrowth of Hierarchical FAU/EMT Zeolites

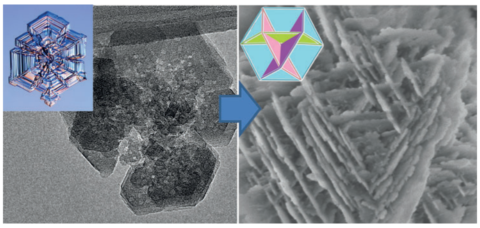

Atypical morphology: Hierarchical faujasite is identified as an intergrowth of FAU and EMT. It is proposed that, under the appropriate growth conditions of faceting and branching, this intergrowth with a very small fraction of EMT, not detectable by XRD, leads to the repetitively branched morphology of faujasite.

Synthetic Methods

N. R. Ball-Jones, J. J. Badillo, N. T. Tran, A. K. Franz* ______ **9462 – 9465**

Catalytic Enantioselective Carboannulation with Allylsilanes

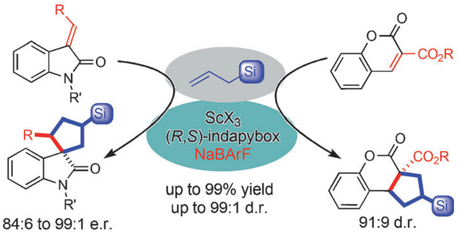

It's a trap: The catalytic asymmetric carboannulation of alkylidene oxindole, coumarin, and malonate substrates with allylsilanes in the presence of a Sc^{III}/BArF/indapybox catalyst affords functionalized cyclopentanes containing a quaternary carbon center with high stereoselectivity. Enantioselective allylation and asymmetric lactone formation by trapping of the β-silyl carbocation are also presented.

Sulfuryl-Based Click Chemistry

J. Dong, K. B. Sharpless,* L. Kwisnek, J. S. Oakdale, V. V. Fokin* ______ **9466 – 9470**

SuFEx-Based Synthesis of Polysulfates

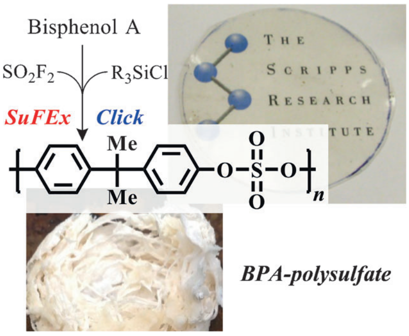

High-molecular-weight polysulfates are readily formed from aromatic bis(silyl ethers) and bis(fluorosulfates) in the presence of a base catalyst. The polymers were obtained in nearly quantitative yield under neat conditions, they are more resistant to chemical degradation than their polycarbonate analogues and exhibit excellent mechanical, optical, and oxygen-barrier properties. BPA = bisphenol A.

Cooperative Biosensors

A. J. Simon, A. Vallée-Bélisle, F. Ricci, H. M. Watkins, K. W. Plaxco* ______ **9471 – 9475**

Using the Population-Shift Mechanism to Rationally Introduce “Hill-type” Cooperativity into a Normally Non-Cooperative Receptor

Natural bioreceptors use cooperativity to improve their sensitivity to subtle changes in ligand concentration. This useful property was rationally engineered into a normally non-cooperative biosensor, significantly enhancing its responsiveness (see picture). The ability to rationally engineer cooperativity should prove useful in applications such as biosensors, molecular logics, and responsive materials.

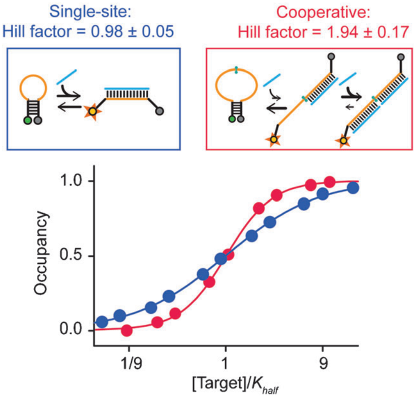

Cyclophanes

Y. Wu, M. Frasconi, D. M. Gardner,
P. R. McGonigal, S. T. Schneebeli,
M. R. Wasielewski,*
J. F. Stoddart* ____________ **9476 – 9481**

Electron Delocalization in a Rigid Cofacial Naphthalene-1,8:4,5-bis(dicarboximide) Dimer

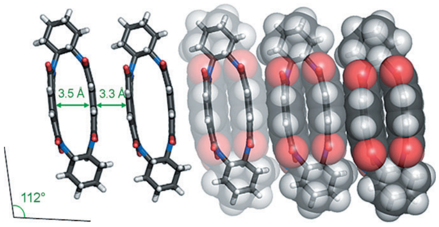

Two are better than one: A doubly-bridged naphthalene diimide (NDI) cyclophane has been synthesized. It shows efficient π-orbital overlap between two rigid cofacial NDI units. The resulting through-space electronic delocalization in the neutral as well as reduced states induces emergent photophysical, electrochemical, and magnetic properties both in solution and in the solid phase.

Methane Conversion

Y.-X. Zhao, Z.-Y. Li, Z. Yuan, X.-N. Li,
S.-G. He* ____________ **9482 – 9486**

Thermal Methane Conversion to Formaldehyde Promoted by Single Platinum Atoms in $PtAl_2O_4^-$ Cluster Anions

One atom is enough: The negatively charged oxide cluster $PtAl_2O_4^-$ is an active species in thermal methane conversion. The single platinum atom activates methane and delivers two hydrogen atoms to the “oxide support” $Al_2O_4^-$. Methane is then transformed to formaldehyde with a high selectivity.

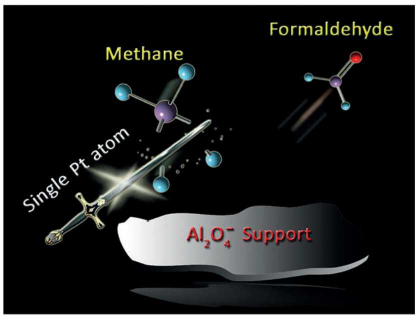

Electroactive Cell Surfaces

A. Pulsipher, D. Dutta, W. Luo,
M. N. Yousaf* ____________ **9487 – 9492**

Cell-Surface Engineering by a Conjugation-and-Release Approach Based on the Formation and Cleavage of Oxime Linkages upon Mild Electrochemical Oxidation and Reduction

Rewired for assembly on demand: Cell surfaces were tailored with bioorthogonal switchable hydroquinone groups by liposome–cell fusion for chemoselective conjugation with aminooxy-tethered cells by mild electrochemical oxidation and release by electrochemical reduction (see scheme). The modulation of cell–cell interactions in this way enabled the generation of 3D tissue structures.

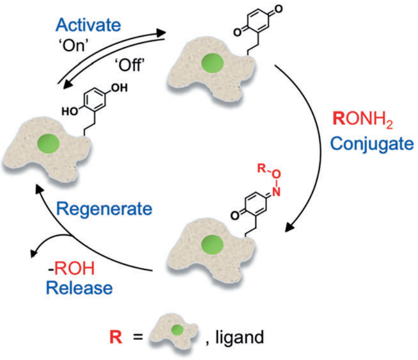

Catalyst Stability

P. Munnik, M. E. Z. Velthoen,
P. E. de Jongh, K. P. de Jong,*
C. J. Gommes* ____________ **9493 – 9497**

Nanoparticle Growth in Supported Nickel Catalysts during Methanation Reaction—Larger is Better

Mind the breakage: The conversion of CO and H_2 to CH_4 over Ni catalysts suffers from particle growth through $[Ni(CO)_4]$-mediated Ostwald ripening. By varying the size and distance of the Ni particles, the size was found to be key: Small 3–4 nm particles grow to large inactive particles, breaking the pore structure of the silica support, while medium 8–9 nm particles remain confined by the pores resulting in stable catalysts.

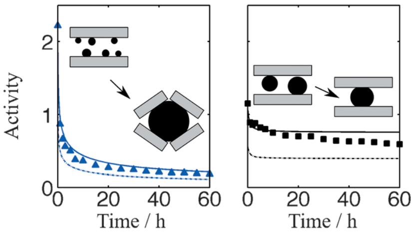

Lithium-Ion Batteries

D. X. Liu, J. Wang, K. Pan, J. Qiu,
M. Canova, L. R. Cao,*
A. C. Co* ________________ 9498 – 9502

In Situ Quantification and Visualization of Lithium Transport with Neutrons

An in-depth study: In situ neutron depth profiling has been demonstrated to provide temporal and spatial measurement of Li concentration and visualization of its transposition upon charging and discharging of a Li-ion cell (see picture). The delithiation process shows the removal of Li near the surface, which leads to a decreased coulombic efficiency.

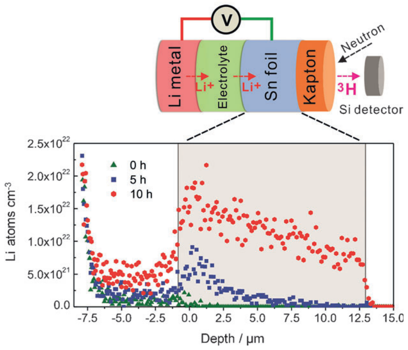

Metal-Free Catalysis

W. H. He, C. H. Jiang, J. B. Wang,
L. H. Lu* ________________ 9503 – 9507

High-Rate Oxygen Electroreduction over Graphitic-N Species Exposed on 3D Hierarchically Porous Nitrogen-Doped Carbons

Spotlighting nitrogen: Preferential exposure of graphitic-N species (GNs) on the surface of bi-continuous N-doped carbon (NC) films that feature hierarchically porous frameworks has been achieved. This unique design was used to identify the catalytic nature of GNs which paves the way to developing highly active metal-free NC electrocatalysts for oxygen reduction.

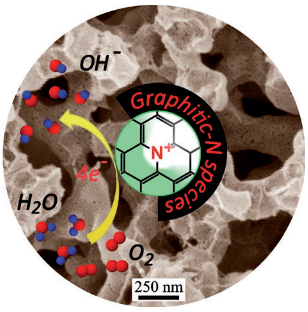

Second Messenger

S. Capolicchio, H. Wang, D. T. Thakor,
S. B. Shears, H. J. Jessen* __ 9508 – 9511

Synthesis of Densely Phosphorylated Bis-1,5-Diphospho-*myo*-Inositol Tetrakisphosphate and its Enantiomer by Bidirectional P-Anhydride Formation

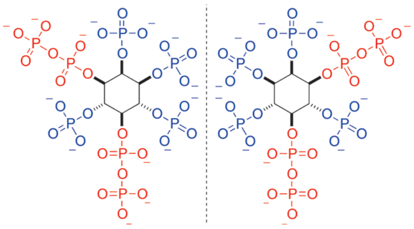

Fully charged: Highly charged bis-diphosphoinositol tetrakisphosphates can be prepared in enantiomerically pure form. These synthetically challenging molecules have the most congested 3D array of phosphates known. The absolute configuration of the two enantiomers is shown by X-ray analysis of the two compounds individually soaked into crystals of the kinase domain of human diphosphoinositol pentakisphosphate kinase 2 (PPIP5K2^{KD}).

Heterogeneous Catalysis

J.-S. Yu, Y.-L. Liu, J. Tang, X. Wang,*
J. Zhou* ________________ 9512 – 9516

Highly Efficient "On Water" Catalyst-Free Nucleophilic Addition Reactions Using Difluoroenoxysilanes: Dramatic Fluorine Effects

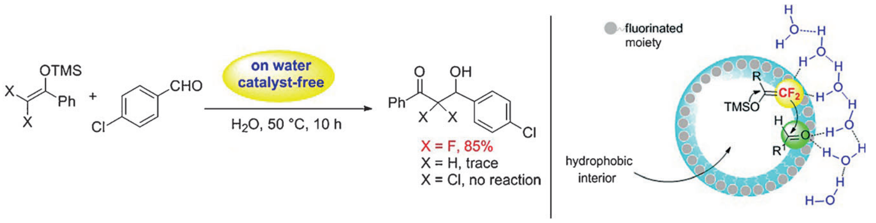

It's on! The C–F···H–O interactions between suitably fluorinated nucleophiles and a hydrogen-bond network at the phase boundary of an oil droplet facilitate "on water" catalyst-free reactions. Accordingly, the title reaction of difluoroenoxysilanes with aldehydes, activated ketones, and isatylidene malononitriles was developed, thus leading to α,α-difluoro-β-hydroxy ketones and quaternary oxindoles.

Doped Ceria

S. Buyukkilic, S. Kim,*
A. Navrotsky* ______ **9517 – 9521**

Defect Chemistry of Singly and Doubly Doped Ceria: Correlation between Ion Transport and Energetics

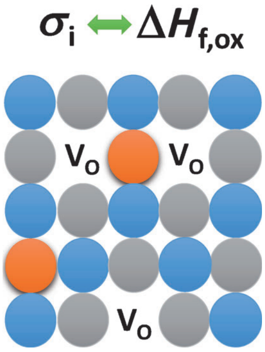

A unique correlation: The correlation between the energetics and the ionic conductivity, σ_i, of ceria that was singly or doubly doped with neodymia and samaria has now also been confirmed for high temperatures. The maximum formation enthalpy of the oxide solid solution, $\Delta H_{f,ox}$, coincides with the maximum σ_i at/near dopant fractions of 0.10, 0.15, and 0.20 in $Ce_{1-x}Nd_xO_{2-0.5x}$, $Ce_{1-x}Sm_xO_{2-0.5x}$, and $Ce_{1-x}Sm_{0.5x}Nd_{0.5x}O_{2-0.5x}$, respectively.

DNA Analogues

A. Pathigoolla,
K. M. Sureshan* ______ **9522 – 9525**

Synthesis of Triazole-linked Homonucleoside Polymers through Topochemical Azide–Alkyne Cycloaddition

Crystals go click: Modified DNA analogues are attractive materials for applications in many fields, however, the synthesis of DNA analogues by conventional methods is difficult owing to poor yield and efficiency and tedious purification. A highly homogeneous, enzyme-stable, crystalline ssDNA analogue was synthesized regiospecifically in quantitative yield through single-crystal-to-single-crystal azide–alkyne cycloaddition polymerization of a modified nucleoside.

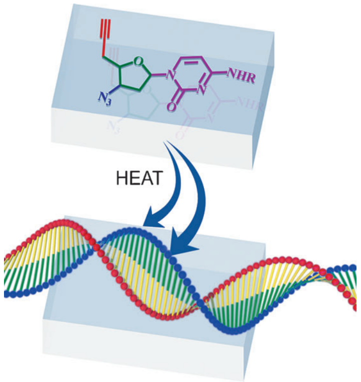

Functional Materials

H. Sun, X. You, Y. Jiang, G. Guan, X. Fang, J. Deng, P. Chen, Y. Luo,
H. Peng* ______ **9526 – 9531**

Self-Healable Electrically Conducting Wires for Wearable Microelectronics

Wires with a will to survive: Self-healable conducting wires were developed by coating electrically conducting carbon nanotubes on the surface of polymer fibers. The wires were used to fabricate wire-shaped supercapacitors, whose high specific capacitance of 140.0 $F\,g^{-1}$ or 1.34 $mF\,cm^{-1}$ was restored after breakage to 92% by self-healing.

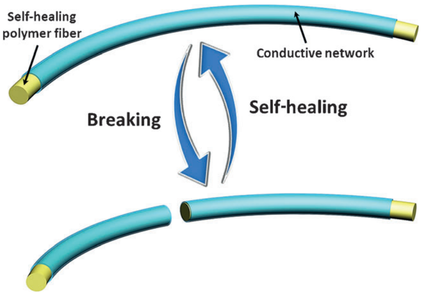

Nanoparticle Adsorption

M. N. O'Brien, B. Radha, K. A. Brown,
M. R. Jones, C. A. Mirkin* __ **9532 – 9538**

Langmuir Analysis of Nanoparticle Polyvalency in DNA-Mediated Adsorption

Stuck on Au: A model system is defined that allows the quantification of nanoparticle adsorption energy under conditions that satisfy the assumptions of the Langmuir adsorption model. This advance could enable fundamental studies of nanoparticles relating to adsorption chemistry, biological processes, and materials by design.

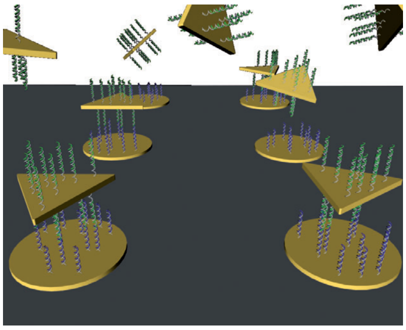

Natural Products

Y. Shi, B. Yang, S. Cai,
S. Gao* ———————— **9539 – 9543**

Total Synthesis of Gracilamine

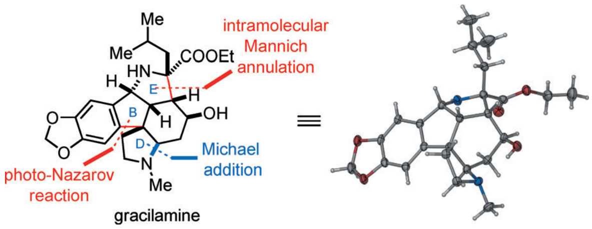

Simple building blocks were employed in the total synthesis of gracilamine, a pentacyclic *Amaryllidaceae* alkaloid. The synthesis features a mild photo-Nazarov reaction, intramolecular 1,4-addition, and an intramolecular Mannich reaction. This strategy provides a novel approach to prepare gracilamine derivatives and structurally related natural products.

Cancer Therapeutics

J. Tian, L. Ding, H. Ju,* Y. Yang, X. Li,
Z. Shen, Z. Zhu J.-S. Yu,*
C. J. Yang* ———————— **9544 – 9549**

A Multifunctional Nanomicelle for Real-Time Targeted Imaging and Precise Near-Infrared Cancer Therapy

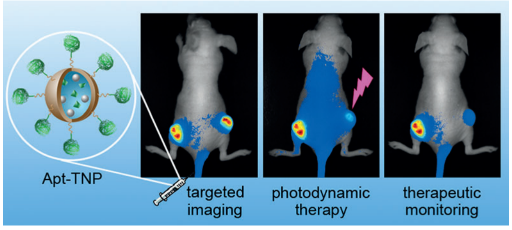

All in one: A lysosome-aimed multifunctional nanomicelle (Apt-TNP) was developed by integrating a target-cell-specific aptamer, a pH-activatable fluorescent probe, and a near-infrared photosensitizer. Apt-TNP enables simultaneous cancer imaging, photodynamic therapy, and real-time self-feedback of therapeutic efficacy.

Tumor Imaging

J. Gallo, N. Kamaly, I. Lavdas, E. Stevens,
Q.-D. Nguyen, M. Wylezinska-Arridge,
E. O. Aboagye,* N. J. Long* **9550 – 9554**

CXCR4-Targeted and MMP-Responsive Iron Oxide Nanoparticles for Enhanced Magnetic Resonance Imaging

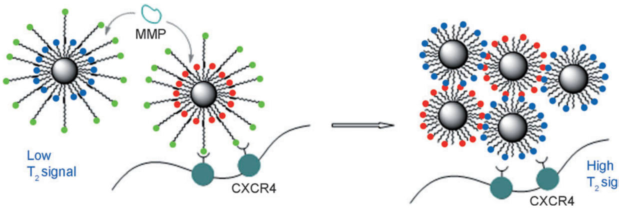

Cleave and cluster: Iron oxide nanoparticles were produced that display azide (red) or alkyne (blue) groups masked by PEG-linked tumor-targeting peptides (green) that bind to the CXCR4 receptor. Matrix metalloproteinases (MMPs) in the tumor microenvironment specifically cleave the peptide linker at the base of the PEG moiety to expose the cross-reactive azide and alkyne groups. This leads to the assembly of clusters and thus to an enhancement of the MRI signal.

Asymmetric Catalysis

F. Zhou, G.-J. Cheng, W. Yang, Y. Long,
S. Zhang, Y.-D. Wu, X. Zhang,*
Q. Cai* ———————— **9555 – 9559**

Enantioselective Formation of Cyano-Bearing All-Carbon Quaternary Stereocenters: Desymmetrization by Copper-Catalyzed N-Arylation

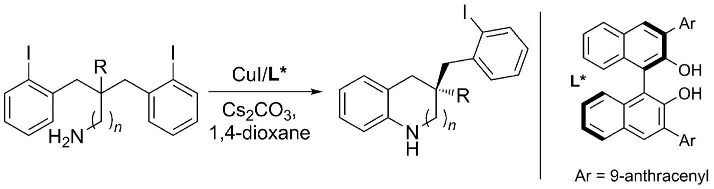

Playing center: An enantioselective formation of cyano-bearing all-carbon quaternary stereocenters in 1,2,3,4-tetrahydroquinolines and 2,3,4,5-tetrahydro-1*H*-benzo[*b*]azepines by the title reaction was developed. A cyano group at the prochiral center played a key role for the high enantioselectivity and worked as an important functional group for further transformations.

Water Structuring

R. Scheu, B. M. Rankin, Y. Chen,
K. C. Jena, D. Ben-Amotz,
S. Roke* ______ **9560 – 9563**

Charge Asymmetry at Aqueous Hydrophobic Interfaces and Hydration Shells

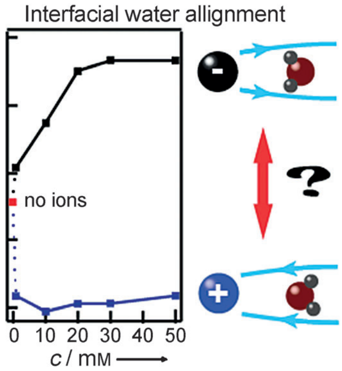

Guilty as charged: Water is often modeled as a dielectric continuum, but the molecular structure of water is asymmetric. Two ions that have a virtually identical size, shape, and structure, but an opposite charge sign have been investigated to see whether charge makes a fundamental difference to water structuring. The spectroscopic data for the hydration and interface structures are found to be remarkably different for opposite charges.

Single-Layer Materials

L. R. Xu, X. Zhou, W. Q. Tian, T. Gao,
Y. F. Zhang, S. B. Lei,*
Z. F. Liu ______ **9564 – 9568**

Surface-Confined Single-Layer Covalent Organic Framework on Single-Layer Graphene Grown on Copper Foil

Co-condensation between benzene-1,3,5-tricarbaldehyde and *p*-phenylenediamine on a graphene surface leads to a surface covalent organic framework (COF) with single-layer thickness. Strong coupling between the surface COF and graphene was confirmed by the significant mixing of states and the relatively large interaction energy revealed by STM and DFT simulation.

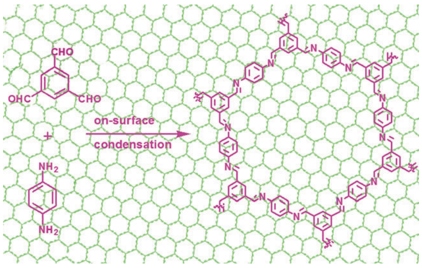

Carbones

T. Morosaki, T. Suzuki, W. W. Wang,
S. Nagase, T. Fujii* ______ **9569 – 9571**

Syntheses, Structures, and Reactivities of Two Chalcogen-Stabilized Carbones

Inside Cover

Carbodichalcogenuranes: New carbones of the type $Ph_2E{\rightarrow}C{\leftarrow}SPh_2(NMe)$ [E = S (**1**) or Se (**2**)] were synthesized and characterized. The carbone **2** can be used to generate a doubly protonated dication and a C-metalated trication with silver(I) and thus provide the first experimental proof of carbodichalcogenurane behaving as a four-electron donor ligand.

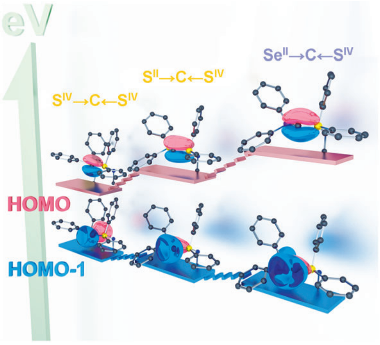

Ruthenium Catalysis

Y. Wang, Z. Zheng,
L. Zhang* ______ **9572 – 9576**

Ruthenium-Catalyzed Oxidative Transformations of Terminal Alkynes to Ketenes By Using Tethered Sulfoxides: Access to β-Lactams and Cyclobutanones

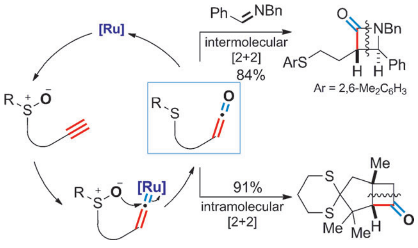

Oxidant included: The oxidation of in situ generated Ru vinylidenes with the help of tethered sulfoxides results in the net transformation of terminal alkynes to valuable ketenes. They undergo characteristic ketene [2+2] cycloaddition reactions with tethered alkenes and external imines, yielding synthetically versatile bicyclic cyclobutanones and β-lactams.

Nanostructures

J. Tian, Q. Liu, N. Cheng, A. M. Asiri, X. Sun* ______ **9577 – 9581**

Self-Supported Cu_3P Nanowire Arrays as an Integrated High-Performance Three-Dimensional Cathode for Generating Hydrogen from Water

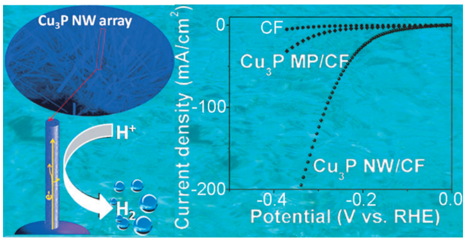

Down to the wire: Self-supported Cu_3P nanowire arrays on porous copper foam (Cu_3P NW/CF) were derived from topotactic low-temperature phosphidation of its $Cu(OH)_2$ NW/CF precursor. As an integrated hydrogen-evolving cathode, Cu_3P NW/CF exhibits excellent catalytic activity and durability with nearly 100% Faradaic efficiency in acidic aqueous electrolytes.

Palladium Catalysis

Z. Lian, S. D. Friis, T. Skrydstrup* ______ **9582 – 9586**

Palladium-Catalyzed Carbonylative α-Arylation of 2-Oxindoles with (Hetero)aryl Bromides: Efficient and Complementary Approach to 3-Acyl-2-oxindoles

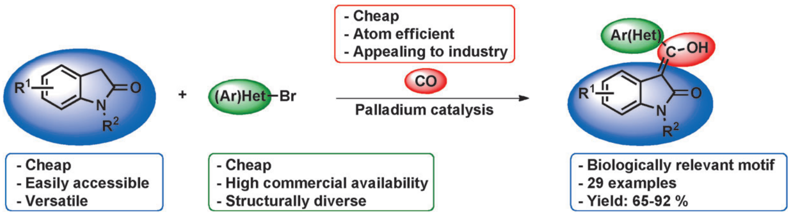

Carbonylate it! 3-Acyl-2-oxindoles are directly obtained through an efficient Pd-catalyzed carbonylative α-arylation of 2-oxindoles with aryl and heteroaryl bromides. Only a mild base is required for the deprotonation and good to excellent yields are obtained even with heteroaromatic substrates.

Kinetics

S. Karmakar, A. Datta* ______ **9587 – 9591**

Tunneling Assists the 1,2-Hydrogen Shift in N-Heterocyclic Carbenes

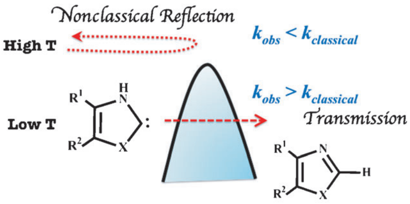

Tunnel vision: Reactions such as 1,2-hydrogen shifts in N-heterocyclic carbenes with small barriers are shown to exhibit exotic quantum mechanical phenomena such as nonclassical reflections at ambient experimental conditions. A small barrier also leads to smaller kinetic isotope effects because of efficient quantum mechanical tunneling of both H and D.

Zeolites

F.-J. Chen, Y. Xu, H.-B. Du* **9592 – 9596**

An Extra-Large-Pore Zeolite with Intersecting 18-, 12-, and 10-Membered Ring Channels

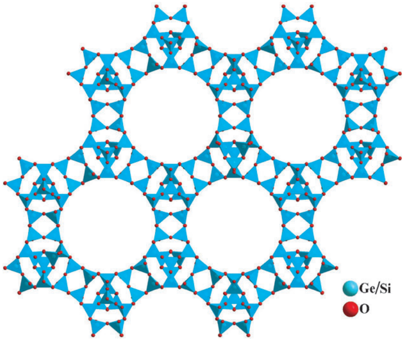

Extra-large-pore molecular sieves: An extra-large-pore zeolite (NUD-1) was synthesized by using an approach based on supramolecular self-assemblies of small aromatic organic structure-directing cations (see picture). The zeolite possesses interconnecting 18-, 12-, and 10-membered ring channels, built from the same building units as those of the zeolites ITQ-33 and ITQ-44.

Glycosides

B. Xu, L. Unione, J. Sardinha, S. Wu,
M. Ethève-Quelquejeu, A. Pilar Rauter,
Y. Blériot, Y. Zhang, S. Martín-Santamaría,
D. Díaz, J. Jiménez-Barbero,*
M. Sollogoub* ________ **9597 – 9602**

gem-Difluorocarbadisaccharides: Restoring the *exo*-Anomeric Effect

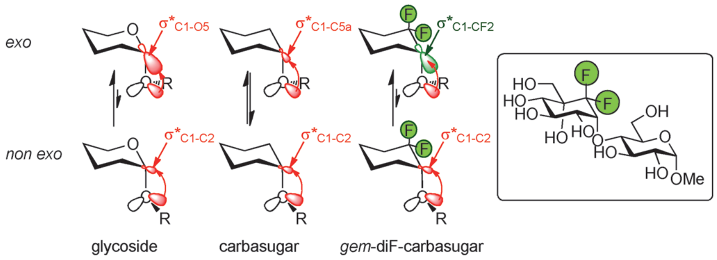

Taking effect: The combination of chemical synthesis, NMR methods, and calculations show that it is possible to restore the anomeric effect for an acetal when replacing one of the oxygen atoms by a CF_2 group. This result provides key findings as it strongly suggests the importance of the stereoelectronic component for the anomeric effect, and may open new avenues for sugar-based drug design.

NHC Catalysis

M. T. Hovey, C. T. Check, A. F. Sipher,
K. A. Scheidt* ________ **9603 – 9607**

N-Heterocyclic-Carbene-Catalyzed Synthesis of 2-Aryl Indoles

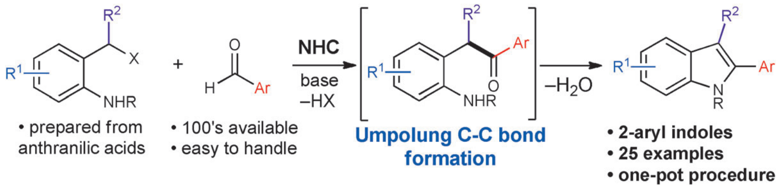

Umpolung: N-heterocyclic carbene catalysis is used for the convergent and efficient transition-metal-free synthesis of 2-aryl-indoles. The interception of a highly reactive and transient aza-*ortho*-quinone methide by an acyl anion equivalent is central to this successful strategy. The reaction exhibits high yields and a wide scope, and it has been applied to a streamlined synthesis of a kinase inhibitor.

O_2 Activation

J. Serrano-Plana, I. Garcia-Bosch,
R. Miyake, M. Costas,*
A. Company* ________ **9608 – 9612**

Selective *Ortho*-Hydroxylation–Defluorination of 2-Fluorophenolates with a Bis(μ-oxo)dicopper(III) Species

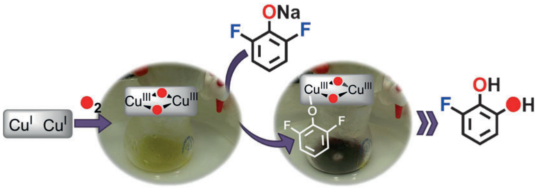

O in, F out: $[Cu^{III}_2(\mu\text{-}O)_2(m\text{-}XYL^{MeAN})]^{2+}$ is a bis(μ-oxo)dicopper(III) species and promotes the electrophilic *ortho*-hydroxylation–defluorination of 2-fluorophenolates to give the corresponding catechols. Isotopic labeling shows that the incoming oxygen atom originates from the bis(μ-oxo) unit. *Ortho*-hydroxylation–defluorination occurs selectively in intramolecular competition with other *ortho*-substituents such as chlorine or bromine.

Organo-Photocatalysis

P. Riente, A. Matas Adams, J. Albero, E. Palomares,* M. A. Pericàs* ——— **9613–9616**

Light-Driven Organocatalysis Using Inexpensive, Nontoxic Bi$_2$O$_3$ as the Photocatalyst

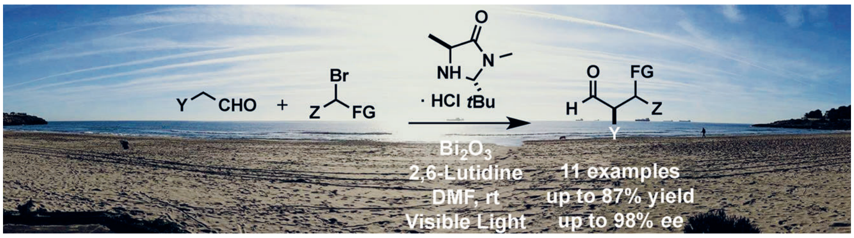

Now it's bismuth time! The asymmetric intermolecular α-alkylation of aldehydes with α-bromocarbonyl compounds can be achieved under visible-light irradiation by combining the second-generation MacMillan catalyst and an inexpensive, nontoxic, and commercially available Bi$_2$O$_3$ powder. This reaction also proceeded with high efficiency when the reaction vial was exposed to the morning sunlight in Tarragona, Spain.

Hypervalent Compounds

A. S. Ivanov, I. A. Popov, A. I. Boldyrev,* V. V. Zhdankin* ——— **9617–9621**

The I=X (X = O,N,C) Double Bond in Hypervalent Iodine Compounds: Is it Real?

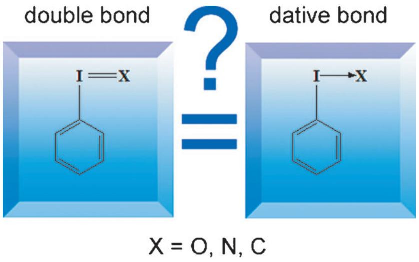

Singled out: The nature of the I=X (X = O, N, C) chemical bonding was examined and compared amongst different hypervalent iodine molecules. The common I=X representation is questioned by results of chemical bonding analyses which confirm the presence of I→O, I→N, and I→C single dative bonds in such compounds.

Organo Cascade Reactions

S. Bera, R. C. Samanta, C. G. Daniliuc, A. Studer* ——— **9622–9626**

Asymmetric Synthesis of Highly Substituted β-Lactones through Oxidative Carbene Catalysis with LiCl as Cooperative Lewis Acid

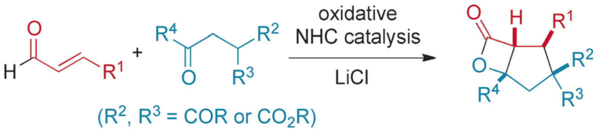

Highly substituted β-lactones are generated by NHC catalysis of enals with β-diketones, β-ketoesters, and malonates bearing a β-oxyalkyl substituent at the α-position. LiCl acts as cooperative Lewis acid. The organocascade comprises two C–C bond formations and one C–O bond formation. Up to four contiguous stereogenic centers including two fully substituted stereocenters are formed with high diastereo- and enantioselectivity.

C–N Coupling

I. Mena, M. A. Casado,* V. Polo, P. García-Orduña, F. J. Lahoz, L. A. Oro* ——— **9627–9631**

C–NH$_2$ Bond Formation Mediated by Iridium Complexes

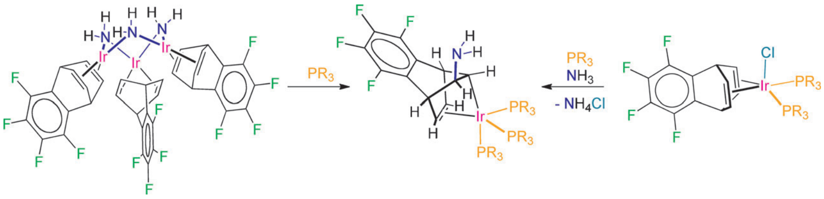

Making C–NH$_2$ bonds: [Ir–NH$_2$] fragments can effect a nucleophilic attack to a coordinated olefin, thereby forming a C–NH$_2$ bond under mild conditions. This reaction follows a bimolecular mechanism induced by the high nucleophilicity of the amido moiety. Alternatively, a discrete chloro complex is able to activate ammonia by forming a C–NH$_2$ bond with a coordinated olefin.

Asymmetric Synthesis

Z. Yu, R. J. Ely, J. P. Morken* **9632 – 9636**

Synthesis of (+)-Discodermolide by Catalytic Stereoselective Borylation Reactions

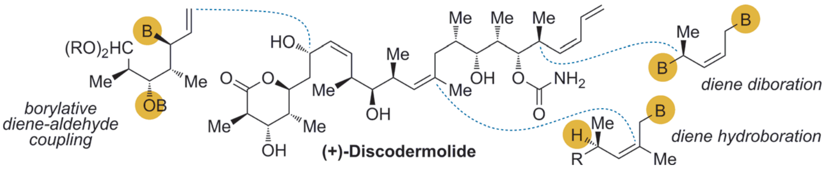

Borylation-based synthesis: The development of a strategy for stereocontrol in catalytic diene hydroboration enables the synthesis of a critical building block for the assembly of (+)-discodermolide. Combined with asymmetric catalytic diboration, hydroformylation, and borylative aldehyde–diene coupling reactions, (+)-discodermolide could then be prepared from simple hydrocarbon-based building blocks.

Metathesis

T. Kasahara, Y. J. Jang, L. Racicot,
D. Panagopoulos, S. H. Liang,
M. A. Ciufolini* **9637 – 9639**

Iodonium Metathesis Reactions

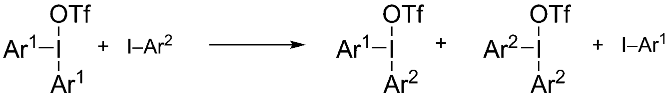

$$\mathrm{Ar^1{-}\overset{OTf}{\underset{Ar^1}{I}}} + \mathrm{I{-}Ar^2} \longrightarrow \mathrm{Ar^1{-}\overset{OTf}{\underset{Ar^2}{I}}} + \mathrm{Ar^2{-}\overset{OTf}{\underset{Ar^2}{I}}} + \mathrm{I{-}Ar^1}$$

Mixed diaryliodoniumtriflates are obtained through treatment of aryl iodides with diaryliodonium triflates. A possible mechanism for the metathesis reaction is proposed.

Synthetic Methods

L. Souillart, N. Cramer* **9640 – 9644**

Highly Enantioselective Rhodium(I)-Catalyzed Carbonyl Carboacylations Initiated by C–C Bond Activation

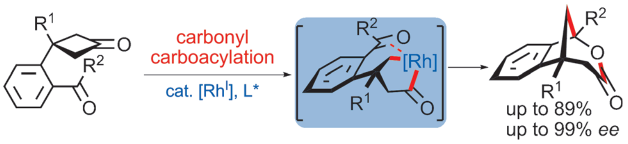

Delivering the goods: Asymmetric carbonyl carboacylations of aldehydes and ketones provide access to functionalized bicyclic lactones. The rhodium(I)-catalyzed transformation is induced by an enantiotopic C–C bond activation of a cyclobutanone and the transient rhodacyclic adds across an appended carbonyl group to deliver the lactones in excellent enantioselectivities.

Polymerization Catalysis

D. E. Babushkin,* V. N. Panchenko,
H.-H. Brintzinger* **9645 – 9649**

Zirconium Allyl Complexes as Participants in Zirconocene-Catalyzed α-Olefin Polymerizations

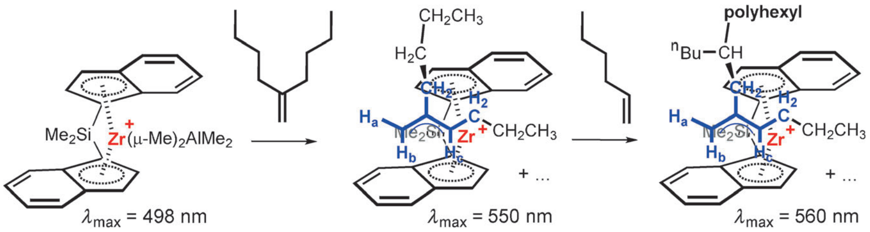

A combination of UV/Vis and NMR spectrometric methods reveals that polymer-carrying cationic Zr allyl complexes derived by β-hydride and subsequent proton abstraction from a Zr polymeryl cation make up about 90% of the catalyst content when 1-hexene is polymerized with a cationic *ansa*-zirconocene catalyst at 25 °C.

C–H Activation

D.-G. Yu, F. de Azambuja, T. Gensch,
C. G. Daniliuc, F. Glorius* 9650–9654

The C–H Activation/1,3-Diyne Strategy: Highly Selective Direct Synthesis of Diverse Bisheterocycles by Rh^{III} Catalysis

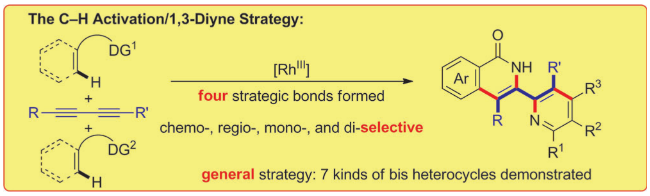

Di-verse: The use of the C–H activation/1,3-diyne general strategy allowed the challenges of selectivity (chemo-, regio-, and mono-/diannulation) to be overcome. This allowed direct construction of diverse polysubstituted bisheterocycles, which are highly important but difficult to access, through the formation of four strategic bonds with high efficiency and high selectivity.

Bioorthogonal Imaging

C. Denk, D. Svatunek, T. Filip, T. Wanek,
D. Lumpi, J. Fröhlich, C. Kuntner,*
H. Mikula* 9655–9659

Development of a ^{18}F-Labeled Tetrazine with Favorable Pharmacokinetics for Bioorthogonal PET Imaging

Inside Back Cover

In vivo click and PET it! A low-molecular-weight radiolabeled tetrazine derivative was prepared by direct [^{18}F]-fluorination (see structure on the left in the figure). PET/MR imaging revealed fast and homogenous biodistribution including in the brain (right). PET/MR = positron emission tomography/magnetic resonance.

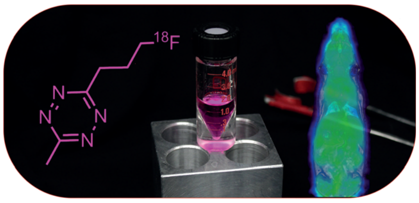

Protein Mass Spectrometry

M. van de Waterbeemd, P. Lössl,
V. Gautier, F. Marino, M. Yamashita,
E. Conti, A. Scholten,
A. J. R. Heck* 9660–9664

Simultaneous Assessment of Kinetic, Site-Specific, and Structural Aspects of Enzymatic Protein Phosphorylation

Back Cover

Comprehensive monitoring of protein phosphorylation: Phosphate incorporation is a universal modification of cellular proteins with multiple functional implications. The combination of native and "bottom-up" mass spectrometry makes it possible to simultaneously visualize dynamic noncovalent protein interactions, identify phosphorylated amino acids, and quantify all occurring phosphoisoforms to generate kinetic data.

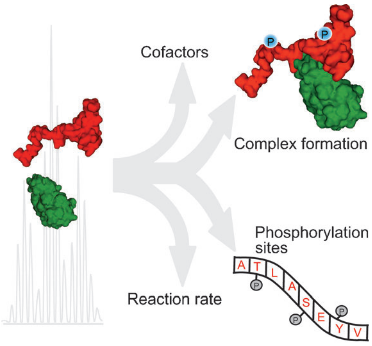

Energetic Materials

T. M. Klapötke,* M. Rusan,
J. J. Sabatini* 9665–9668

Chlorine-Free Pyrotechnics: Copper(I) Iodide as a "Green" Blue-Light Emitter

Out of the blue: A suitable blue-light-emitting pyrotechnic with low sensitivities to various ignition stimuli has been developed without the need to employ chlorine-containing materials. With copper(I) iodide proven as a suitable blue-light emitter in pyrotechnics, the risk of generating highly carcinogenic polychlorinated aromatic compounds during the combustion process is eliminated.

Supramolecular Switches

The thermal and light-induced photoisomerization of bifunctional azobenzene–oligoglycerol conjugates was examined in solution and on supramolecularly functionalized gold nanoparticles and planar gold surfaces. The wettability of the functionalized gold surfaces could be reversibly switched with light. Thermal half-lives of *Z*-isomers were determined for different environments to provide information about the stability of the functional switches for further applications.

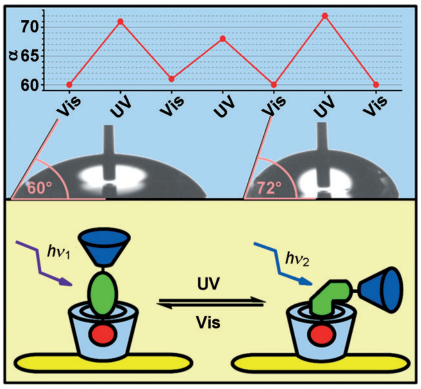

Supporting information is available on www.angewandte.org (see article for access details).

A video clip is available as Supporting Information on www.angewandte.org (see article for access details).

This article is available online free of charge (Open Access).

This article is accompanied by a cover picture (front or back cover, and inside or outside).

The Very Important Papers, marked VIP, have been rated unanimously as very important by the referees.

The Hot Papers are articles that the Editors have chosen on the basis of the referee reports to be of particular importance for an intensely studied area of research.